

Electronic and optical properties of monolayer TiS₃: DFT calculation

A. H. FIROUZKHANI^a, M. VAEZ-ZADEH^{a,*}, H. JAMNEZHAD^a, M. BERAHMAN^b

^aFaculty of Physics, K. N. Toosi University of Technology, Tehran, Iran

^bDepartment of Electrical and Computer Engineering, Graduate University of Advanced Technology, Kerman, Iran

The present study aimed to investigate the properties of Monolayer TiS₃. The novel properties such as high mobility, facile synthesis, non-toxic, and cost-effective, candidate Monolayer TiS₃ as a suitable replacement for Phosphorene, MoS₂, MoSe₂, and Graphene. Inclusive applications in optics and electronics tempt researchers to study TiS₃ by experiments and calculations. In this work, the electrical properties were calculated, and then optical properties like dielectric function, reflectivity, absorption and refraction, extinction coefficient, optical conductivity, electron energy loss function were investigated. Results show monolayer TiS₃ is non-magnetic, and it can be used in high frequency in UV devices, polarizer in a different direction for specified frequencies, as a frequency selector, and valuable device in analyzers applications.

(Received December 13, 2019; accepted December 7, 2020)

Keywords: Monolayer TiS₃, Optical properties, Transition metal trichalcogenides, Density functional theory, Polarizers, UV devices, Frequency selector

1. Introduction

Graphene introduces a new branch of materials which are known as two dimensional (2d) materials. These materials have gained considerable interest for their remarkable potentials in Nano electronic and optic. Whereas graphene shows remarkable mobility, low bandgap limited its application in current semiconductor devices. Bringing other 2d materials such as transition metal dichalcogenide family [1-5] to light may solve that problem. Monolayers of MoS₂ satisfy desire bandgap; however, field-effect transistors (FETs) based on the MoS₂ monolayer show low mobility [5]. Phosphorene monolayer with bandgap around 0.3 eV to 1.5 eV, exhibited high mobility about 104 cm²/V/s. high reactivity of Phosphorene makes it unstable then need protection in applications [6-8]. Therefore, cost-effective replacement is needed, which can satisfy quick exfoliating from bulk, proper bandgap, and high mobility. These crystals called Transition metal trichalcogenides (TMTCs) with chemical MX₃ formula where M is transition metal, and X is S, Se or Te.

Recently in TMTCs family, TiS₃ has attracted many attentions due to non-toxic, easy synthesis and low-cost monolayer production [9]. Monolayers TiS₃ grow as ribbon and it is considered as the n-Type device with on/off ratios of 104 and mobilities less than 73 cm²V⁻¹s⁻¹ by high photo response less than 2910 AW⁻¹ [10-12]. Electrical properties show high values of the thermoelectric coefficient (-0.7mV/K), Hall mobilities (10-50 cm²/V·s), donor densities (1018-1019 cm⁻³) and conductivities of 10- 20 (mΩ ·cm)⁻¹ at ambient temperature [10].

Monolayer TiS₃ apply in cathodes of batteries and thermoelectric conversion devices [10]. Since both sulfur

and titanium have low weight and cost, they are very suitable for hydrogen stores [13]. Additionally, Monolayer TiS₃ are used in optoelectronics [11] as well as solar cell devices [10]. Furthermore, acceptable light absorption, introduce TiS₃ as a component in the material of nano optical waveguide polarizer's. [11, 14].

So far many literatures have investigated properties of monolayer TiS₃. Jin et al. shows by the change from bulk to monolayer, TiS₃ bandgap goes to direct manner. Also changing the number of layers will change the bandgap [14]. Gorochov et al. have reported results on TiS₃ single crystals photoresponse in aqueous media that show TiS₃ single crystal is unstable in aqueous acidic and basic solutions [10]. By STM and photo electrochemical measurements, Molina-Mendoza et al. reported that TiS₃ nanoribbons have a bandgap of 1.2 eV [13]. In addition, contrary to molybdenum and tungsten dechalchogenide (with direct bandgap just at the single-layer) TiS₃ has a direct bandgap which is optimum for photovoltaic and photo catalysis applications [10-11, 15-16].

Many studies have been done on monolayer TiS₃. However, less attention has been paid to the analytical properties of Monolayer TiS₃ in waveguide polarizers. In this work, the DFT calculation computes the optical properties of monolayers TiS₃.

2. Experimental (Method, Optimization)

By LDA approximation, the energy of the electrons density was estimated by the energy of a constant local density. However, it was failed in situations where the density undergoes rapid changes such as in molecules. To solve this problem, the gradient of the electron density is being used, the so-called Generalized Gradient Approximation (GGA). In this calculation WIEN2k code

[17] with LAPW method (GGA) as powerful software was used. To solve Kohn Sham equations, it is necessary to set some parameters in software. They are muffin-tin (MT) spheres radii, convergence parameter, k-points. MT valued 2.48 and 1.96 a.u. for Ti and S, respectively, convergence parameter (RMT.Kmax) was chosen as 7.0, in this context, Kmax refers to maximum k vector in-plane wave expansion, and RMT indicates minimum radii of the atomic sphere. Lmax was used 10 as lattice parameter in the MT. Self-consistency calculation by 1000 k points in Brillouin Zone (BZ) was done. Once total energy

converged to 0.0001 electron charge, the iteration was stopped.

Bulk geometry has been considered as a starting point from ref [18]. Optimization calculation gives bond length for Ti-S 2.48 Å, 2.48 Å, and 2.45 Å. Also, the PBE optimized lattice constant are $a=5.03$ Å, $b=3.45$ Å, $c=39.9$ Å, and angle is 96.49° . As can be seen in Table 1, these parameters are in good agreement with previous reports and are compared with experimental data. The optimized unit cell of monolayer TiS_3 in the monoclinic phase has been illustrated in Fig 1.

Table 1. Optimized crystal calculation summary, the optimization calculations give the bond length values for Ti-S as 2.48 Å, 2.48 Å and 2.45 Å, optimized lattice constant by PBE are $a=5.03$ Å, $b=3.45$ Å and $c=39.9$ Å, and angle is 96.49° , aRef. [19]. bRef. [20]. cRef. [21]

	a (Å)	b (Å)	β	Ti-S (Å)
current work	5.03	3.45	96.49°	2.48, 2.48, 2.45
Ref. [19]	5.04	3.43	-	2.46, 2.50, 2.67
Ref. [20]	4.98 ^b	3.39 ^b	97.04°	-
Ref. [21]	4.95 (Expt)	3.40 (Expt)	96.56° (Expt)	-

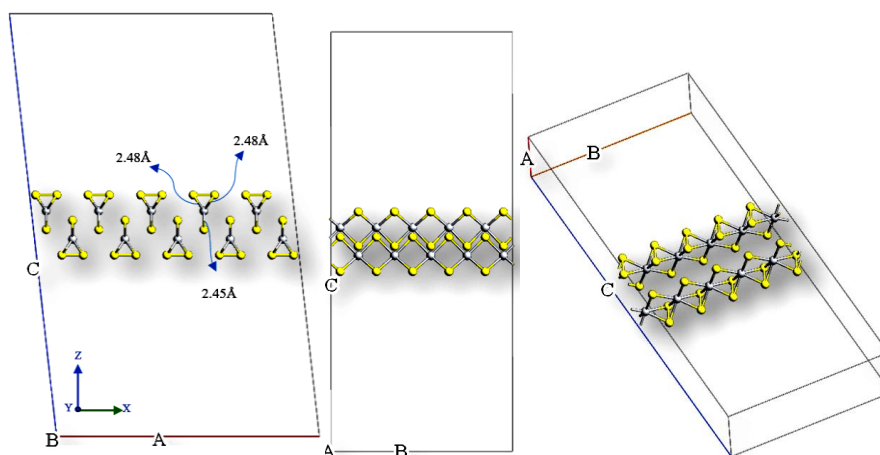


Fig. 1. Optimized monolayer of TiS_3 in different views. Unit cell of monolayer TiS_3 in the monoclinic phase (color online)

3. Results and discussion

Electronic band structure or distribution of energy in term of valence and conduction bands, reveals novel information about electronics characteristic of material in which clarify conductivity/semiconductivity (p-type/n-type)/dielectric. Therefore, this is very valuable to study band structure more accurately. GGA calculation gives bandgap 0.19 eV, in order to estimate the U values in the GGA +U calculation, we take into account an adjustable phenomenological routine in which theoretical bandgap match with experimental one. Therefore, the U value is chosen 7 eV. The bandgap was calculated for the GGA+U method and result in 1.12 eV. Fig 2 (a). Shows band structure by GGA+U calculation. Table 2 shows different bandgap in different approaches in literatures. This bandgap shows good agreement with experimental and

other computational approach [22] and proves monolayer TiS_3 is a semiconductor.

For more consideration, it is required to study parameters that in which shows spin, orbital transitions, and status of bindings. The density of states (DOS) satisfies this requirement. As the first step in this context, and for GGA+U approach, total DOS of monolayer TiS_3 was calculated in Fig. 2 (b). For values greater than zero, the spin of electrons is up and for the others is down. Since total DOS of Monolayers TiS_3 is symmetric, means the non-magnetic nature of Monolayers TiS_3 , which is in good agreement with previous reports [19].

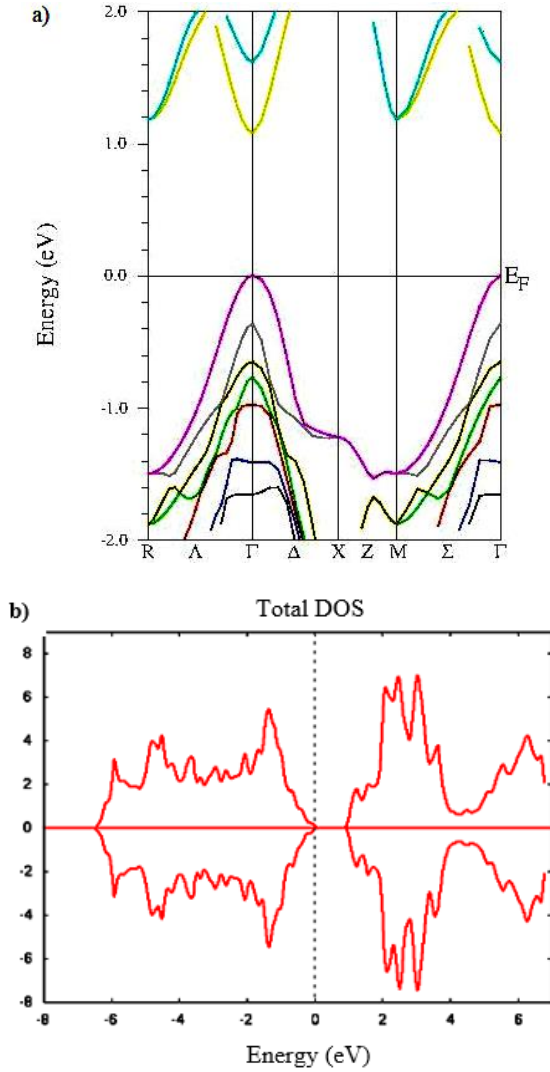


Fig. 2. a) Band structure of Monolayer TiS₃ using the GGA+U approximation, was calculated resulted in 1.12 eV, this band gap shows good agreement with experimental data and proves monolayer TiS₃ is a semiconductor. b) Calculated total DOS of Monolayer TiS₃. Fermi energy is aligned to zero, total DOS of Monolayers TiS₃ is symmetric, means the non-magnetic nature of Monolayers TiS₃ (color online)

Table 2. Experimental and theoretical bandgap of monolayers TiS₃ [22]

Property	This work GGA+U(eV)	Ref.[22] HSE06(eV)	This work PBE(eV)	Ref.[22] Expt(eV)
Γ-Γ	1.12	1.12	0.19	~ 0.9

For more details about bindings, orbitals, and engineering atoms total DOS is no longer useful, so it is needed to calculate partial DOS (PDOS) (see Fig. 3)

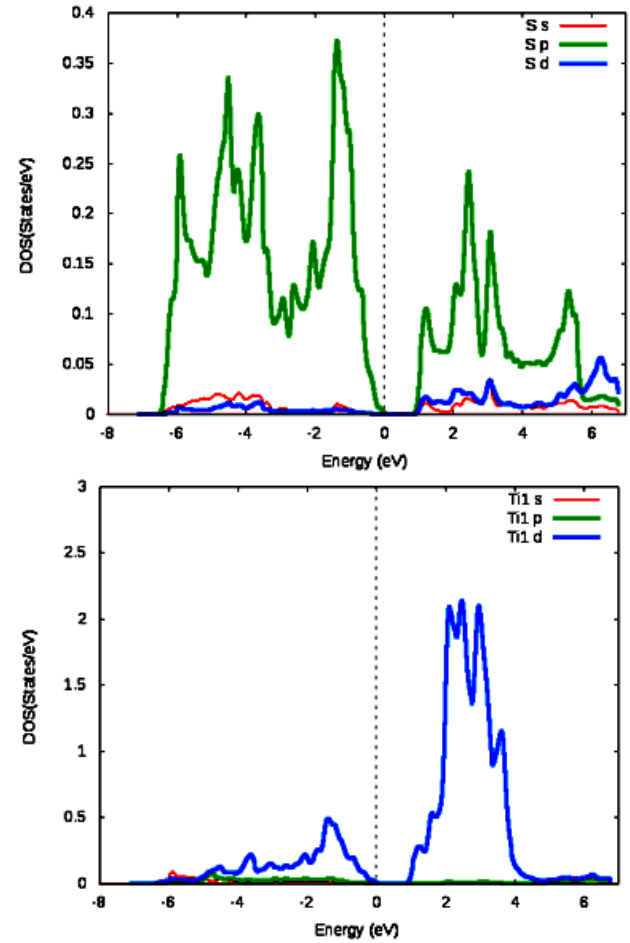


Fig. 3. Calculated total PDOS of S (a) and Ti (b) atom in monolayer TiS₃ unit cell. Fermi energy is aligned to zero. Electrons for Values less than zero participate in bonding, and others play carrier role in conductivity. The density of states in Fig. 3, shows that 3p-orbitals in S-atoms, make chemical bonds with 3d orbitals in Ti-atoms (color online)

Electrons for Values less than zero participate in bonding, and others play carrier role in conductivity. The density of states in Fig. 3, shows that 3p-orbitals in S-atoms, make chemical bonds with 3d orbitals in Ti-atoms. In energy between -6.5eV to 0 eV, states of S-3p and Ti-3d form bonds with a width of about 6.5 eV in the GGA+U method. Band structure shows Monolayer TiS₃ is a direct-gap semiconductor.

As a start point for entering to study of optical properties, dielectric function is used to describe the response of a material to the electromagnetic field. This function is defined as:

$$\varepsilon(\omega) = \varepsilon_1(\omega) + \varepsilon_2(\omega) \quad (1)$$

The imaginary part is specified by [23-24]:

$$\varepsilon_2(\omega) = \left(\frac{4\pi^2 e^2}{m^2 \omega^2} \right) \sum_{i,j} \int \langle i | M | j \rangle^2 f_i (1 - f_j) \times \delta(E_{j,k} - E_{i,k} - \omega) d^3 k \quad (2)$$

where M is dipole matrix and f_i is Fermi distribution. By Kramer's- Kronig relation, the real part can be extracted from an imaginary part:

$$\varepsilon_1(\omega) = 1 + \frac{2}{\pi} P \int_0^\infty \frac{\omega' \varepsilon_2(\omega') d\omega'}{\omega'^2 - \omega^2} \quad (3)$$

For $\varepsilon_1(\omega) < 0$ waves are not propagated, so absorption and loss have not happened, a low quantity of ε_2 represent Intra-band absorption, and high quantity shows Inter-band absorption. The imaginary and real parts of the dielectric function for Monolayer TiS_3 in the GGA+U method were calculated for energies to 14eV. Fig. 4 shows the real and imaginary part of the dielectric function of monolayers TiS_3 , in all directions of x, y, z, the same trend was seen.

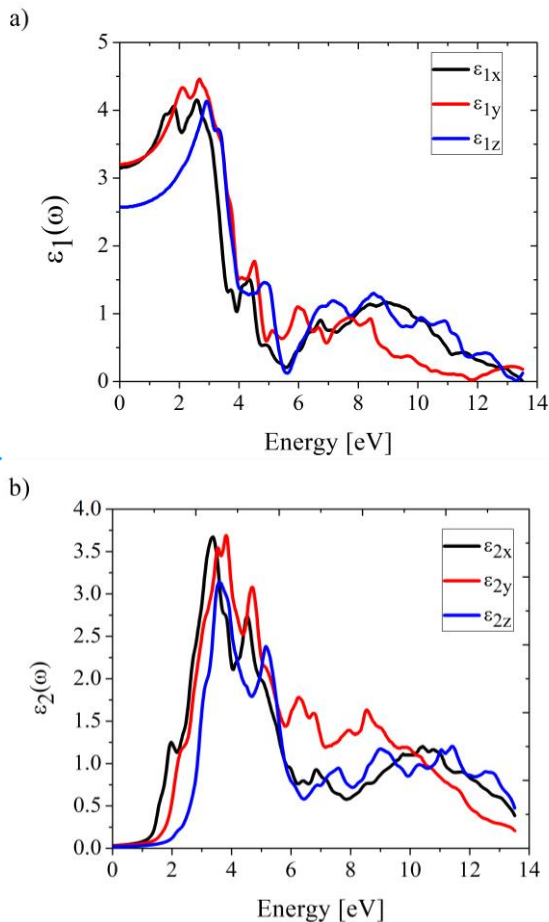


Fig. 4. Calculated a real and b imaginary parts of dielectric function for Monolayer TiS_3 , the peak in Fig. 4, located in the ultraviolet area, introduces monolayer TiS_3 as appropriate device in high-frequency UV application (color online)

By dividing Fig. 4a, to 2 spectral sections, it can be studied more accurately. The first section is related to

valence to conduction band transition with bandgap (0-0.5 eV), and waves can be transmitted in plateaued trend. The second region, which is specified by a rapid decrease in the reflectance, is extended between 1.2 and 3eV. In this region by increasing real part, decrease the imaginary part that means more propagation and less absorption. The peak in $\varepsilon_1(\omega)$, in the ultraviolet area, introduce monolayer TiS_3 as appropriate high-frequency UV device applications.

It was seen a peak for in Fig. 4b, related to transitions inter orbitals and represent intense absorption in energy (2 to 6) eV. By partial DOS in Fig. 3, this peak originates from conduction bands to the valence band in Ti-3d to S-3p. For the rest of energy, more than 6 eV, $\varepsilon_2(\omega)$ descend quickly.

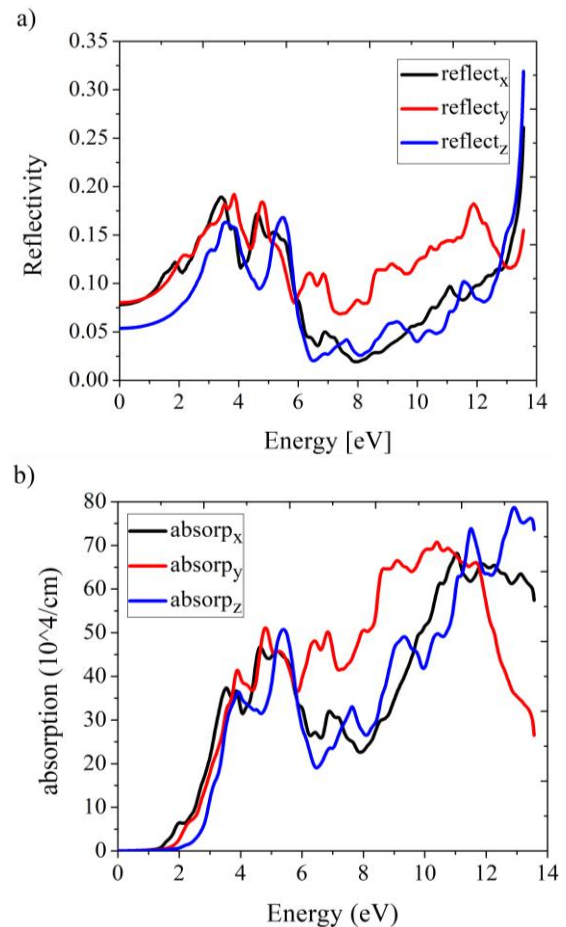


Fig. 5. a) Reflection, b) absorption, more accurate survey shows in energies 3.4 eV, 4.6 eV, 6.9 eV, 11.0 eV for x-direction, and 3.9 eV, 4.8 eV, 6.84 eV, 8.93 eV, 10.3 eV for y-direction, and 5.4 eV, 7.63 eV, and 9.31 eV for z-direction, reflection and absorption are in highest position. This conformity, confirms the application of monolayer TiS_3 as a polarizer in a different direction for specified frequencies (color online)

In Fig. 5, reflectivity and absorption coefficient $\alpha(\omega)$ has been illustrated. The absorption edge appeared around 1.45eV. The maximum Reflectivity for 13.56 eV, i.e., the minimum value ε_1 happen. This conformity is reasonable. Comparing Reflectivity and absorption trend in Fig. 5,

reveals that in energies 0-1.45 eV, Reflectivity is isotropic in x and y-direction. More inspection shows in energies 3.4 eV, 4.6eV, 6.9 eV, 11.0 eV for x-direction and 3.9 eV, 4.8 eV, 6.84 eV, 8.93 eV, 10.3 eV for y-direction and energies, 5.4 eV, 7.63 eV, and 9.31 eV for z-direction, reflectivity and absorption are in highest position. These results confirm the application of monolayer TiS₃ as a polarizer in a different direction for specified frequencies. Moreover, more interesting around 4.5 eV (4.6 – 4.8) in x and y-direction, monolayer TiS₃ is a good reflector while for z-direction in this range, has the lowest quantity it means that with rotating this material frequency can be selected that shows application of monolayer TiS₃ as a frequency selector.

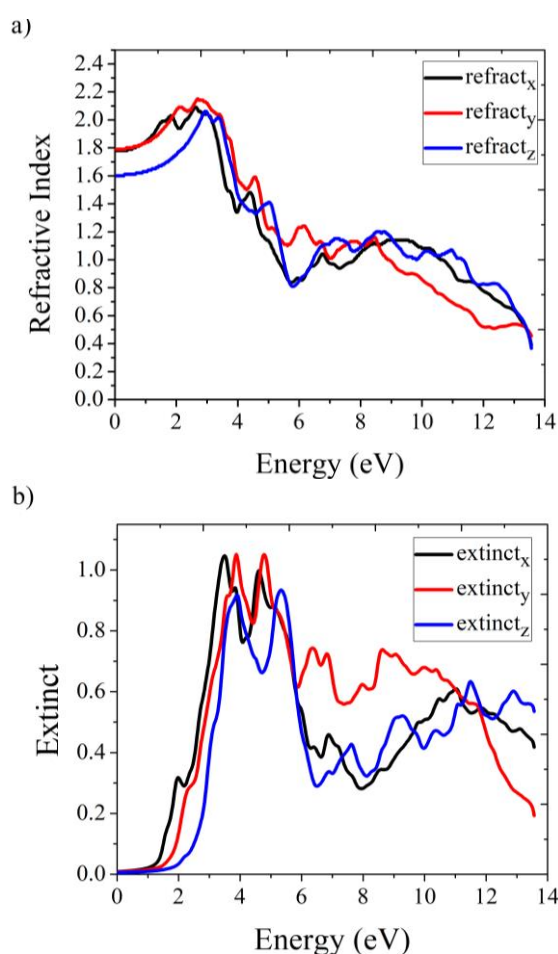


Fig. 6. a) Refractive index, b) Extinction coefficient, the refractive index variation, happen in a transparent area and reaches to peak in UV region at 3 eV. The refractive index has been originated from bonding; a process can increase the electron density. The most striking point in this regard is isotropy from 0 to 1.7 eV for refractivity and is valuable in analyzers applications (color online)

The extinction coefficient and refractive index are calculated in Fig. 6. The refractive index, in lower energies, goes on plateaued trend and goes up synchronized with energy ascending. Static refraction index $n(\omega=0)$ is 1.78 in GGA+U approach. The refractive index variation, happen in a transparent area and reaches

to peak in UV at 3 eV. The refractive index has been originated from bonding; a process can increase the electron density. The most striking point in this regard is isotropy from 0 to 1.7 eV for refractivity and is valuable in analyzers applications.

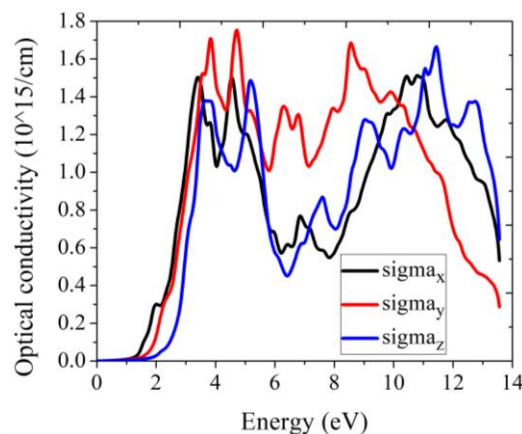


Fig. 7. Optical conductivity spectrum Monolayer TiS₃, since excited electrons have no sufficient energy to travel from the band gap and shift to the conduction band, the optical conduction begins around 1.94 eV (color online)

In Fig. 7, the optical conduction $\sigma(\omega)$, appears in energy around 1.94 eV and change between 1 to 1.8 ($10^{15}/\text{sec}$) for energy (2 to 6) eV. Since excited electrons have no sufficient energy to travel from the bandgap and shift to the conduction band, the optical conduction begins around 1.94 eV.

An exciton consists in a bound state between an electron and a hole, this state can travel in periodic structure of a crystal, in this way can be transported energy but is not able to be transferred charge, whenever photon was attracted by a crystal, force electron transfers from the conduction band to valence band and creates an exciton. TiS excitonic event happens in Fig. 7. For energies between 3 to 5 eV by a transition from Ti-3d conduction band to S-3p valence band.

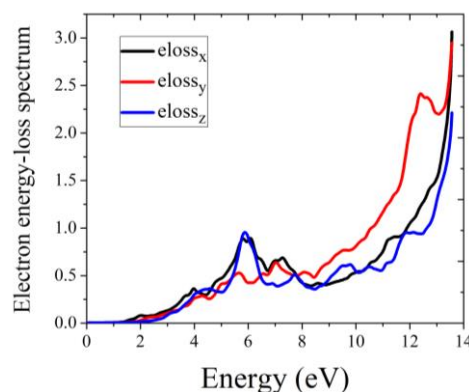


Fig. 8. Electron energy-loss spectrum of Monolayer TiS₃, Plasmonic peak in 13.5eV that is correspond with $\epsilon_1=0$. Calculations show a peak in $\epsilon_1(\omega)$, is in the ultraviolet area and introduces application of monolayer TiS₃ as high-frequency UV device (color online)

As another function which surveys traveling fast electron is Energy Loss function [25] and defined as follow:

$$L(\omega) = \frac{\varepsilon_2(\omega)}{\varepsilon_1^2(\omega) + \varepsilon_2^2(\omega)} \quad (4)$$

Sharp peaks in this function are for Plasmonic frequency. In Fig. 8, the electron energy loss spectrum (EELS) is plotted for Monolayer TiS₃ in monoclinic phase. EELS give valuable information about the charge carrier, plasmons, inter-band, and intraband transitions. Peaks in this quantity are useful to extract parameters [26]. In Fig. 9, the peak in 5.86 eV is related to the transition from Ti-3d to S-3p. In $\varepsilon_1(\omega)=0$ shows plasma resonance. On the other hand, $\varepsilon_1(\omega)$ represents $\varepsilon_1(\omega)=0$ occurs in 13.5 eV which verify plasmonic peaks in EELS.

4. Conclusion

Electrical and optical properties of monolayers TiS₃ has been detected. Band structure studied by GGA+ U and U changed until bandgap matched with experimental results. Total DOS shows non-magnetic properties of monolayers TiS₃, and PDOS shows bonding is related to -5.5 to 0 eV. For conduction bond, the transition happens from Ti-3d to S-3p. Optical conductivity shows excitonic appearance at 3 to 5 eV. There is a plasmonic peak in 13.5eV correspond with $\varepsilon_1=0$. Also, Calculation has been shown a peak in $\varepsilon_1(\omega)$, in the ultraviolet area, introduce monolayer TiS₃ as appropriate high-frequency UV device applications. Matched peaks in Reflectivity and absorption in some frequencies and conformity of peak and trough around 4.5 eV in Reflectivity is promising monolayer TiS₃ as polarizer and frequency selector in specified frequencies.

References

[1] F. F. Zhu, W. J. Chen, X. Yong, C. L. Gao, D. D. Guan, C. H. Liu, D. Qian, S. C. Zhang, J. F. Jia, *Nat. Mater.* **14**, 1020 (2015).
 [2] T. Fang, A. Konar, H. Xing, D. Jena, *Phys Rev B.* **78**, 205403 (2008).
 [3] L. Song, C. Lijie, L. Hao, B. S. Pavel, C. Jin, J. Ni, A. G. Kvashnin, D. G. Kvashnin, J. Lou, I. B. Yakobson, P. M. Ajayan, *Nano Lett.* **10**, 3209 (2010).
 [4] P. Vogt, P. De Padova, C. Quaresima, J. Avila, E. Frantzeskakis, M.C. Asensio, A. Resta, B. Ealet, G. Le Lay, *Phys Rev Lett.* **108**, 155501 (2012).
 [5] J. Dai, M. Li, X. C. Zeng, *Wires Comput. Mol. Sci.* **6**, 211 (2016).

[6] M. Berahman, M.H. Sheikhi, *J Comput Theor Nanos.* **8**, 90 (2011).
 [7] F. Zakerian, M. Berahman, *Opt Quant Electron.* **48**, 370 (2016).
 [8] M. Berahman, M. Asad, M. Sanaee, M. H. Sheikhi, *Opt. Quant. Electron.* **47**, 3289 (2015).
 [9] M. Barawi, E. Flores, I. J. Ferrer, J. R. Ares, *J. Mater. Chem. A.* **3**, 7959 (2015).
 [10] I. J Ferrer, M. D. Maciá, V. Carcelén, J. R. Ares, C. Sánchez, *Energy Proced.* **22**, 48 (2012).
 [11] A. J. Molina-Mendoza, M. Barawi, R. Biele, E. Flores, J. R. Ares, C. Sánchez, G. Rubio Bollinger, N. Agrait, R. D'Agosta, I. J. Ferrer, A. Castellanos-Gomez, *Electron. Mater.* **1**, 1500126 (2015).
 [12] A. Lipatov, P. M. Wilson, M. Shekhirev, J. D. Teeter, R. Netusil, A. Sinitiskii, *Nanoscale* **7**, 12291 (2015).
 [13] M. Barawia, E. Flores, M. Ponthieu, J. R. Ares, F. Cuevas, F. Leardini, I. J. Ferrer, C. Sánchez, *J. Electr. Eng.-Slovak* **3**, 24 (2015).
 [14] Y. Jin, X. Li, J. Yang, *Phys. Chem. Chem. Phys.* **17**, 18665 (2015).
 [15] A. S. Pawbake, J. O. Island, E. Flores, J. R. Ares, C. Sanchez, I. J. Ferrer, S. R. Jadkar, H. S. J. van der Zant, A. Castellanos-Gomez, D. J. Late, *ACS Appl. Mater. Inter.* **7**, 24185 (2015).
 [16] I. J. Ferrer, J. R. Ares, J. M. Clamagirand, M. Barawi, C. Sánchez, *Thin Solid Films* **535**, 398 (2013).
 [17] P. Blaha, K. Schwarz, G. K. H. Madsen, D. Kvasnicka, J. Luitz, R. Laskowsk, F. Tran, L. Marks, *WIEN2k: An Augmented Plane Wave Plus Local Orbitals Program for Calculating Crystal Properties*, Techn. Universitat Vancouver (2019).
 [18] S. Furuseth, L. Brattas, A. Kjekshus, *Acta Chem. Scand. A.* **29**, 623 (1975).
 [19] H. Zheng, M. Zhu, J. Zhang, X. Du, Y. Yan, *RCS Advances* **6**, 55194 (2016).
 [20] J. Kang, L. W. Wang, *Phys. Chem. Chem. Phys.* **18**, 14805 (2016).
 [21] Y Saeed, A. Kachmar, M. A. Carignano, *J. Phys. Chem. C* **121** 1399 (2017).
 [22] J. A. Silva-Guillén, E. Canadell, P. Ordejón, F. Guinea, R. Roldán, *2D Mater.* **4**, 1 (2017)
 [23] C. Ambrosch-Draxl, J. O. Sofo, *Comput. Phys. Commun.* **175**, 1 (2006).
 [24] F. Wooten, *Optical Properties of Solids*, New York, (1972).
 [25] R. E. Humml, *Electronic Properties of Materials*, Springer, College of Engineering, University of Florida Gainesville USA (2011).
 [26] C. J. Powell; J. B. Swan, *Phys. Rev.* **115**, 869 (1959).

*Corresponding author: mehdi@kntu.ac.ir